Dalton Transactions

ROYAL SOCIETY OF CHEMISTRY

PAPER

View Article Online
View Journal | View Issue

Cite this: *Dalton Trans.*, 2025, **54**, 17982

Mechanochemistry unlocking stoichiometric control in alkali metal carboxylate coordination polymers

Michał K. Leszczyński, *[a,b] Iwona Justyniak [a] and Janusz Lewiński *[a,b]

Received 16th August 2025,
Accepted 3rd November 2025

DOI: 10.1039/d5dt01954k

rsc.li/dalton

Alkali metal-based coordination polymers represent a promising alternative to transition metal systems, yet their development remains limited due to the inherent challenges in controlling and predicting the assembly of structures based on alkali cations. In this report we demonstrate a comprehensive study on the preparation of Na, K and Rb 1,3,5-benzenetricarboxylates using both self-assembly in an aqueous solution and the solid-state mechanochemical methods, revealing a remarkable degree of structural diversity in these seemingly simple systems. Notably, the developed mechanochemical procedures enabled excellent control over the metal-to-linker stoichiometry, as demonstrated by the selective formation of two M_2HBTC-type phases (M = K, Rb; BTC = 1,3,5-benzenetricarboxylate), which were not readily accessible by solution-based synthesis. These results demonstrate the unique advantages of mechanochemistry in enabling stoichiometric control and accessing coordination polymers that remain out of reach for conventional solution-based methods.

Introduction

The growing awareness of undesired environmental impacts of chemical processes calls for the development of efficient transformations that would offer reduction of cumbersome steps and the overall use of solvents. This challenge has spurred the renaissance of mechanochemistry in which chemical transformations are effected by mechanical force in the absence of solvents.[1–4] In this regard, mechanochemistry has emerged as a robust and increasingly adopted synthetic approach to organic and inorganic molecular products.[5,6] It is also widely used for synthesis of diverse functional materials, such as metal oxides,[7] metal halide perovskites[8,9] and others, owing to its operational simplicity, reduced reliance on bulk solvents, and ability to access reaction pathways unavailable under conventional conditions. Mechanochemical methods have proven particularly effective in the synthesis of coordination polymers,[10–12] enabling the formation of several archetypal MOFs,[13–19] including drug-loaded MOFs,[20,21] as well as previously unreported MOF polymorphs and metastable structures that are not accessible through solution-based methods.[22–24] Another advantage of mechanochemistry is the potential for precise control over reaction stoichiometry, which can be especially valuable in multicomponent systems (*e.g.* cocrystals, coordination polymers) where solution-based approaches often lead to non-stoichiometric mixtures, kinetic by-products, or phase segregation.[25] For example, mixed-metal MOF-74 materials incorporating bimetallic nodes (selected from: Zn, Mg, Co, Ni, Cu, Ca) in controlled 1 : 1 ratio have been synthesised by mechanochemical route, which were not accessible using solution-based methods.[26] Furthermore, in some cases mechanochemical synthesis has enabled control over the metal-to-linker ratio in coordination polymers, as shown for reaction systems involving Zn/Cd with cyanoguanidine[27] or Ag with ethylenethiourea,[28] yielding coordination polymers that are challenging to prepare *via* solution-based methods. However, such examples remain limited, highlighting the unique yet still underexplored potential of mechanochemistry for precise stoichiometric control in coordination polymer synthesis.

Coordination polymer chemistry, recognized by the 2025 Nobel Prize, has traditionally focused on frameworks built around transition metals, whose directional bonding preferences, variable oxidation states, and ability to form well-defined coordination geometries and discrete clusters facilitate the design of robust extended frameworks. Compared to the transition metal centres, the interactions of alkali metal cations with carboxylate ligands are more ionic, making the structure less rigid and harder to predesign. However, their high natural abundance and low toxicity make alkali metals appealing building units for functional coordination networks, particularly for large-scale and biomedical applications.[29–32]

[a]*Institute of Physical Chemistry Polish Academy of Sciences, Kasprzaka 44/52, 01-224 Warsaw, Poland. E-mail: leszczynski.m@hotmail.com, janusz.lewinski@pw.edu.pl*
[b]*Faculty of Chemistry Warsaw University of Technology, Noakowskiego 3, 00-664 Warsaw, Poland*

The most prominent example of alkali metal-based MOFs is the family of CD-MOFs, originally developed by Stoddart *et al.*[33] using cyclodextrins as organic linkers, with promising application potential in various fields.[34] Furthermore, carboxylate-based coordination polymers using alkali metals as nodes have been applied in drug delivery systems, gas mixture separation, chemical sensors, and electrochemical devices.[29–32]

Moreover, alkali metal-based MOFs serve as excellent templates for porous carbons, as the homogeneous distribution of metal ions ensures uniform dispersion within the carbon matrix upon pyrolysis, promoting the formation of highly porous materials with promising applications in energy storage and catalysis.[35,36] Overall, the inherent properties of the alkali metal-based coordination networks make them a very interesting alternative to classical transition metal-based structures, but their design and efficient application remains a considerable challenge.[29–32] Similarly to the transition metal-based counterparts, the alkali metal-based coordination polymers are usually prepared using solvothermal, hydrothermal or diffusion-based strategies.[29–31] To the best of our knowledge, only two recent reports demonstrated that the mechanochemical approach utilizing simple alkali hydroxides as metal sources can be a very efficient strategy for preparation of alkali metal-based coordination networks.[37,38]

Herein, in the course of our ongoing efforts towards development of wet and mechanochemically driven solid-state synthetic methods of 1D,[39] 2D,[40,41] 3D[19,20] coordination polymers and alkali–metal-based systems in particular,[35] we present a systematic study on the synthesis of alkali metal 1,3,5-benzenetricarboxylates (BTC) involving Na^+, K^+, and Rb^+, employing both low-temperature self-assembly in aqueous solutions and mechanochemical methods. While alkali metal 1,3,5-benzenetricarboxylates have been the focus of earlier, investigations,[42–48] our results demonstrate that their chemistry still holds considerable untapped potential, with many aspects of their formation and structural variability remaining to be elucidated. As a result of our study, a series of four new 2D and 3D coordination polymers were prepared and characterized revealing a striking degree of structural diversity among these deceptively simple systems. Moreover, two additional coordination polymers, previously reported only from solution-based synthesis, were successfully obtained under mechanochemical conditions.[35] Notably, the ability to control the metal-to-linker stoichiometry played a critical role in directing product formation, particularly under mechanochemical conditions (Fig. 1). In two cases, the desired coordination networks could be obtained in high yield only *via* mechanochemical synthesis, as repeated attempts to isolate these phases from solution were unsuccessful or led to impure or low-yield products. These findings underscore the unique capacity of mechanochemistry not only to streamline synthesis under mild and scalable conditions, but also to access stoichiometrically defined coordination polymers that are otherwise inaccessible through conventional solution-based methods.

Experimental section

Materials and methods

All chemicals were purchased from commercial sources and used without further purification. Spectroscopic grade organic solvents and deionized water were used for the syntheses. Mechanochemical reactions were conducted in 10 ml stainless steel reactors equipped with stainless steel balls (10 mm diameter, one ball per reactor). The Retsch MM400 shaker mill was used to conduct the mechanochemical reactions (30 Hz, 20 min). Powder X-Ray Diffraction (PXRD) data were collected on the Empyrean diffractometer (PANalytical) employed with Ni-filtered Cu Kα radiation (40 kV, 40 mA) using Bragg–Brentano geometry and Si zero-background holder. Elemental analyses were carried out with an UNICUBE Elementar Analyser (Elementar GmbH). Scanning Electron Microscopy (SEM) imaging was performed using FEI Nova NanoSEM 450 system equipped with a field emission electron gun operating at 2 kV. Thermogravimetric analysis (TGA) was carried out with the TA Instruments Q600 analyser

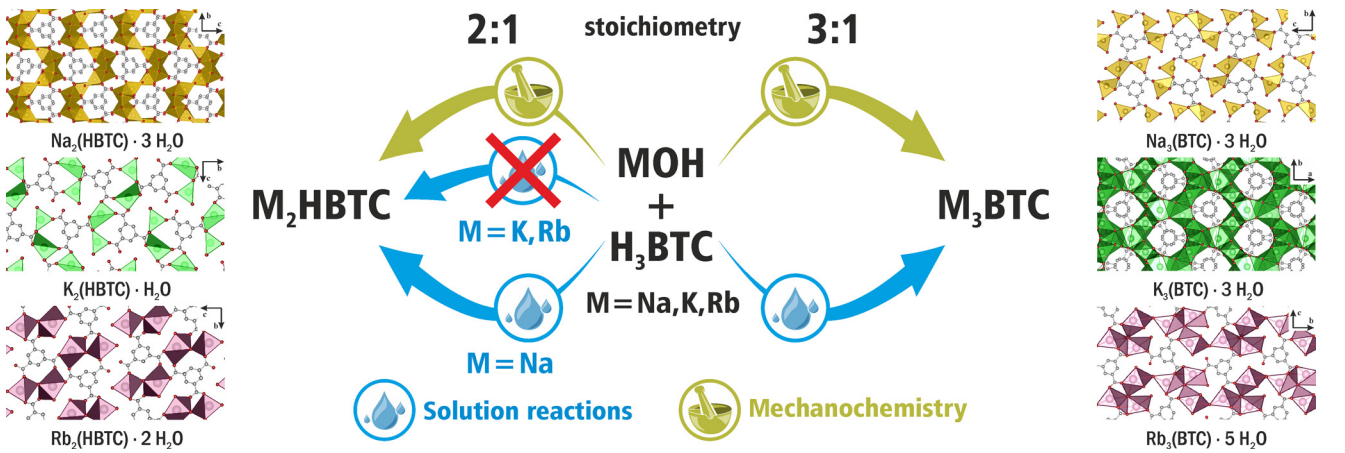

Fig. 1 Conceptual representation of the stoichiometry control in formation of alkali metal-based coordination polymers presented in this report.

(25–1000 °C temperature range) in argon flow (100 mL min^{-1}) in open alumina crucibles.

General procedure for preparation of aqueous M_3BTC solutions (M = Na, K, Rb). Respective MOH (7.14 mmol) was dissolved in 10 ml of water. Next H_3BTC was added (500 mg, 2.38 mmol). The mixture was heated to 50 °C and shaken until the observed pH (tested using standard indicator paper) was close to neutral. Afterwards, the mixture was cooled to the room temperature and filtered.

Synthesis of $Na_3BTC{\cdot}3H_2O$. Solution method has been reported previously.[35] **Mechanochemical method**: NaOH (57 mg, 1.43 mmol) and H_3BTC (100 mg, 0.48 mmol) and DMF (20 μl) were ball milled in a stainless steel jar (20 min, 30 Hz). The resulting $Na_3BTC{\cdot}3H_2O$ powder was washed with acetone and dried. Yield: 149 mg (95%). Elemental analysis (%) found: C 32.80, H 2.79; cacld for the formula $[C_9H_3O_6Na_3{\cdot}3H_2O]$: C 32.74, H 2.75.

Synthesis of $Na_2HBTC{\cdot}3H_2O$. Solution method: Solutions of NaOH (37 mg, 0.96 mmol) 1 ml of water and H_3BTC (100 mg, 0.48 mmol) in 2 ml of EtOH were mixed, which resulted in an immediate precipitation of $Na_2HBTC{\cdot}3H_2O$ as a white solid. The product was separated by centrifugation, washed with acetone and dried. Yield: 132 mg (89%). Elemental analysis (%) found: C 35.01, H 3.31; cacld for the formula $[C_9H_4O_6Na_2{\cdot}3H_2O]$: C 35.08, H 3.27. **Mechanochemical method**: NaOH (38 mg, 0.96 mmol), H_3BTC (100 mg, 0.48 mmol) and H_2O (8 μl, 0.5 mmol) were ball milled in a stainless steel jar (20 min, 30 Hz) yielding $Na_2HBTC{\cdot}3H_2O$ as white powder. Yield: 137 mg (93%). Elemental analysis (%) found: C 35.12, H 3.23; cacld for the formula $[C_9H_4O_6Na_2{\cdot}3H_2O]$: C 35.08, H 3.27.

Synthesis of $K_3BTC{\cdot}3H_2O$. Solution method has been reported previously.[35] **Mechanochemical method**: KOH (80 mg, 1.43 mmol) and H_3BTC (100 mg, 0.48 mmol) were ball milled in a stainless steel jar (20 min, 30 Hz). The resulting mixture was put in a closed glass contained and aged for 30 days resulting in formation of $K_3BTC{\cdot}3H_2O$ as a white powder. Yield: 173 mg (96%). Elemental analysis (%) found: C 28.48, H 2.45; cacld for the formula $[C_9H_3O_6K_3{\cdot}3H_2O]$: C 28.56, H 2.40.

Synthesis of $K_2HBTC{\cdot}H_2O$. KOH (54 mg, 0.96 mmol) and H_3BTC (100 mg, 0.48 mmol) and DMF (20 μl) were ball milled in a stainless steel jar (20 min, 30 Hz). The resulting $K_2HBTC{\cdot}H_2O$ powder was washed with acetone and dried. Yield: 134 mg (92%). Elemental analysis (%) found: C 35.48, H 2.01; cacld for the formula $[C_9H_4O_6K_2{\cdot}H_2O]$: C 35.51, H 1.99.

Synthesis of $Rb_3BTC{\cdot}5H_2O$. Solution method: To the aqueous Rb_3BTC solution (2 ml, 0.24 M) 10 ml of iPrOH was added, which resulted in immediate precipitation of $Rb_3BTC{\cdot}5H_2O$ as white solid. The product was separated by centrifugation, washed with acetone and dried. Yield: 236 mg (89%). Elemental analysis (%) found: C 19.49, H 2.41; cacld for the formula $[C_9H_3O_6Rb_3{\cdot}5H_2O]$: C 19.52, H 2.37. **Mechanochemical method**: RbOH (147 mg, 1.44 mmol), H_3BTC (100 mg, 0.48 mmol) and EtOH (20 μl) were ball milled in a stainless steel jar (20 min, 30 Hz). The resulting $Rb_3BTC{\cdot}5H_2O$ powder was washed with acetone and dried. Yield: 255 mg (96%). Elemental analysis (%) found: C 19.50, H 2.34; cacld for the formula $[C_9H_3O_6Rb_3{\cdot}5H_2O]$: C 19.52, H 2.37.

Synthesis of $Rb_2HBTC{\cdot}2H_2O$. RbOH (98 mg, 0.96 mmol) and H_3BTC (100 mg, 0.48 mmol) and DMF (20 μl) were ball milled in a stainless steel jar (20 min, 30 Hz). The resulting $Rb_2HBTC{\cdot}2H_2O$ powder was washed with acetone and dried. Yield: 187 mg (94%). Elemental analysis (%) found: C 26.09 H 1.93; cacld for the formula $[C_9H_4O_6Rb_2{\cdot}2H_2O]$: C 26.04, H 1.95.

X-ray structure determination of alkali metal-based coordination compounds. The single crystals of, $Na_2HBTC{\cdot}3H_2O$, $K_2HBTC{\cdot}H_2O$, $Rb_3BTC{\cdot}5H_2O$ and $Rb_2HBTC{\cdot}2H_2O$ were selected under Paratone-N oil, mounted on the nylon loops and positioned in the cold stream on the diffractometer. The SCXRD data were processed with CrysAlisPro, Data Collection and Processing Software for Agilent X-ray Diffractometers.[49] The structures $Na_2HBTC{\cdot}3H_2O$, $K_2HBTC{\cdot}H_2O$, $Rb_3BTC{\cdot}5H_2O$ and $Rb_2HBTC{\cdot}2H_2O$ were solved by direct methods using the SHELXT program and were refined by full matrix least-squares on F^2 using the program SHELXL.[50] implemented in the OLEX2[51] or WinGX[52] suite. All non-hydrogen atoms were refined with anisotropic displacement parameters. H atoms on C atoms were added to the structure model at geometrically idealized coordinates and refined as riding atoms. H atoms of H_2O molecules were located from a Fourier map (Tables S1–S7). Crystallographic data (excluding structure factors) for the structure reported in this paper have been deposited with the Cambridge Crystallographic Data Centre as a supplementary publication. CCDC 2359250 ($Na_2HBTC{\cdot}3H_2O$), 2359252 ($K_2HBTC{\cdot}H_2O$), 2450580 ($Rb_3BTC{\cdot}5H_2O$) and 2359487 ($Rb_2HBTC{\cdot}2H_2O$).

Results and discussion

Following our previous report on the use of alkali 1,3,5-benzenetricarboxylates as precursors to porous materials with promising applications in energy storage,[35] we wondered if similar alkali metal-based coordination networks could be prepared using different metal : linker ratio *via* solution or mechanochemical approach.

Sodium-BTC networks

Initially, we investigated the mechanochemical preparation of the Na-BTC reaction system in order to verify the accessibility of the previously reported $Na_3BTC{\cdot}3H_2O$[35] phase. In this regard, a series of mechanochemical reactions involving NaOH and H_3BTC (3 : 1 molar ratio) were conducted under various conditions (neat grinding or liquid-assisted grinding (LAG) using EtOH or DMF, see Table S5 and Fig. S2). While all of those attempts allowed for preparation of the desired $Na_3BTC{\cdot}3H_2O$ phase, the DMF LAG procedure was most favourable due to increased phase purity and crystallinity of the product as evidenced by the PXRD data. Encouraged by the successful preparation of $Na_3BTC{\cdot}3H_2O$, we explored further mechanochemical transformations aimed at preparation of product with different stoichiometry by grinding NaOH with H_3BTC in 2 : 1 ratio,

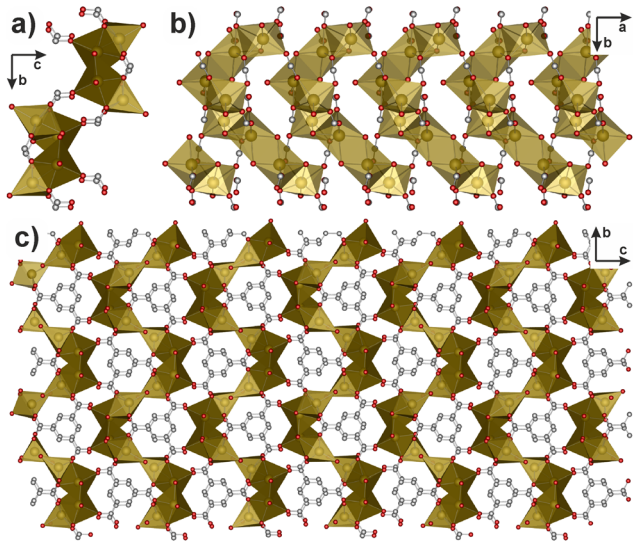

Fig. 2 Crystal structure of $Na_2HBTC{\cdot}3H_2O$: 2D polymeric SBU (a and b), 3D coordination network (c). Na = yellow, O = red, C = grey, H atoms have been omitted for clarity. Single crystals of $Na_2HBTC{\cdot}3H_2O$ were prepared from concentrated aqueous Na_3BTC solution at RT.

which resulted in the preparation of a new 2 : 1 coordination network $Na_2HBTC{\cdot}3H_2O$ (Fig. 2) as a white microcrystalline powder. The high-quality single crystals of $Na_2HBTC{\cdot}3H_2O$ could be grown from concentrated aqueous solution of Na_3BTC at room temperature, which highlights the role of acid–base equilibria in directing product composition within the studied reaction system. Furthermore, we found that $Na_2HBTC{\cdot}3H_2O$ phase could also be directly precipitated by mixing aqueous solution of NaOH and EtOH solution of H3BTC (2 : 1 molar ratio, Fig. S1d, see the Experimental part and SI for more details). Notably, this compound can also be readily converted into the $Na_3BTC \cdot 3H_2O$ phase by simple grinding with one equivalent of NaOH, as evidenced by PXRD (Fig. S2e).

The SCXRD investigations of $Na_2HBTC{\cdot}3H_2O$ showed that it forms a 3D supramolecular structure and crystallizes in $P2_12_12_1$ space group (Table S1). All of the metal cations in $Na_2HBTC{\cdot}3H_2O$ are coordinated by 5 or 6 oxygen atoms from organic linker or solvent molecules. The SBUs structures in $Na_2HBTC{\cdot}3H_2O$, form extended 2D layered structures perpendicular to the crystallographic *a* axis (Fig. 2a and b). Finally, the layered SBUs are linked by the BTC molecules, forming extended 3D structure (Fig. 2c).

Potassium-BTC networks

Having demonstrated the formation of $Na_3BTC{\cdot}3H_2O$ and $Na_2HBTC{\cdot}3H_2O$ in both solution and solid state we followed the course of investigation towards products involving heavier cations: K and Rb. As demonstrated in our previous report, the K_3BTC solution prepared by reaction of KOH with H_3BTC (3 : 1 eq.) could be used for precipitation of $K_3BTC{\cdot}3H_2O$ phase by introduction of organic solvent.[35] However, in the course of our investigations we found that small amount of another product: $K_2HBTC{\cdot}H_2O$ can also be crystallised upon exposition of the aqueous K_3BTC solution to MeOH vapours. Despite considerable efforts including room temperature and hydrothermal reactions conducted in various stoichiometries, no high-yielding procedure of $K_2HBTC{\cdot}H_2O$ preparation from solution was established. Instead, the $K_3BTC{\cdot}3H_2O$ phase is preferably formed in most synthetic attempts. Nevertheless, efficient preparation of $K_2HBTC{\cdot}H_2O$ was possible by application of the mechanochemical approach (see the Mechanochemistry study below).

The structural investigation of the $K_2HBTC{\cdot}H_2O$ using SCXRD showed that it forms a 3D coordination network crystallised in $P2_1/c$ space group (Table S2). All of the potassium cations in $K_2HBTC{\cdot}H_2O$ are coordinated by 6 oxygen atoms. The metal centres in $K_2HBTC{\cdot}H_2O$ are linked by the carboxylate groups forming 1D SBU chains extending in the direction of the *a* crystallographic axis (Fig. 3a and b). The BTC linkers interconnect the 1D SBUs in $K_2HBTC{\cdot}H_2O$ into the 3D coordination network (Fig. 3c).

In order to investigate the possibility of $K_3BTC{\cdot}3H_2O$ and $K_2HBTC{\cdot}H_2O$ preparation in the solid state, we have conducted a mechanochemical screening involving reactions in various stoichiometries and conditions (for details see Table S5 and Fig. S3, S4). Consequently, we have established that the $K_2HBTC{\cdot}H_2O$ phase can be prepared *via* a DMF LAG process involving KOH and H_3BTC in 2 : 1 molar ratio. In the case of $K_3BTC{\cdot}3H_2O$, we found that while it can be prepared directly by mechanochemical processes (neat grinding or LAG), the products were not phase-pure (Fig S4a–c). To overcome this

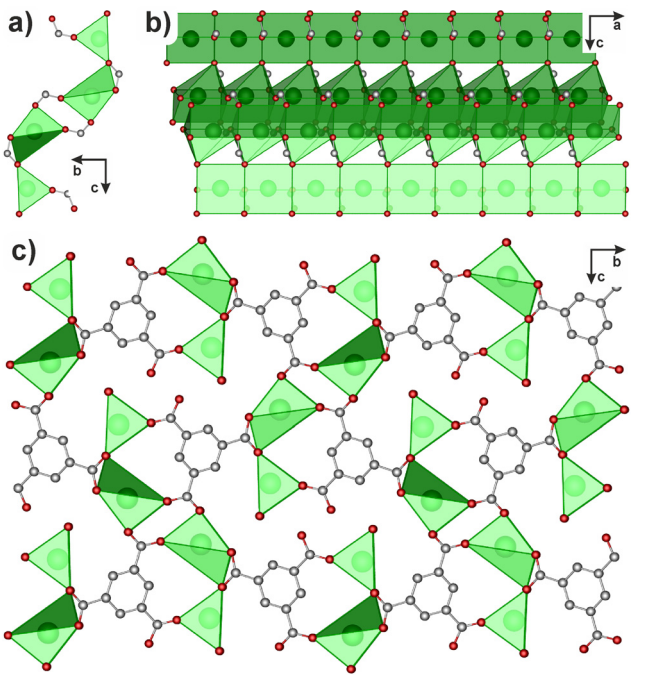

Fig. 3 Crystal structure of $K_2HBTC{\cdot}H_2O$: 1D polymeric SBU (a and b), 3D coordination network (c). K = green, O = red, C = grey, H atoms have been omitted for clarity. Single crystals of $K_2HBTC{\cdot}H_2O$ (mixed with single crystals of $K_3BTC{\cdot}3H_2O$) were prepared by exposition of aqueous K_3BTC solution to MeOH vapours at RT.

limitation, we studied the post-synthetic treatment of the mechanochemical products of KOH and H_3BTC reaction (the 3 : 1 molar ratio), leading to the conclusion that pure $K_3BTC{\cdot}3H_2O$ phase can be prepared either by simple aging (30 days, Fig. S4d) or DMF soaking (2 days, Fig. S4e). Interestingly, the aging-related recrystallisation can be directly observed by Scanning Electron Microscopy (SEM) displaying clear changes in crystal size an morphology (Fig. S17 and S18). Furthermore, we found that the $K_2HBTC{\cdot}H_2O$ phase can be easily transformed to $K_3BTC{\cdot}3H_2O$ in the solid state by grinding with addition of KOH and H_2O (the 1 : 1 : 1 molar ratio, Fig. S4g).

Rubidium-BTC networks

Extending the scope of our investigations towards rubidium we observed significant similarities with regard to the potassium-based systems discussed above as well as in the previous report.[35] Initially the reaction involving RbOH and H_3BTC (3 : 1 molar ratio) in water was performed, yielding Rb_3BTC solution. After addition of iPrOH to the Rb_3BTC solution, $Rb_3BTC{\cdot}5H_2O$ immediately formed as white precipitate, which could also be prepared as high quality single crystals by exposing the aqueous Rb_3BTC solution to the iPrOH vapours, as confirmed using PXRD (Fig. S6) and SCXRD (Table S3) analyses. Moreover, we found that upon exposure of the aqueous Rb_3BTC solution to EtOH vapours small amount of single crystals of $Rb_2HBTC{\cdot}3H_2O$ can be obtained. Despite several attempts, we did not succeed in establishing a procedure for selective preparation of $Rb_2HBTC{\cdot}3H_2O$ from solution in satisfactory yield, but it could be easily prepared *via* mechanochemical strategy, similarly to the potassium-based network $K_2HBTC{\cdot}H_2O$ (see the discussion of the Mechanochemical experiments below).

The SCXRD of the $Rb_3BTC{\cdot}5H_2O$ single crystals revealed that it forms a closely packed 3D coordination network in $P2_1$ space group (Table S3). The coordination geometry around the Rb^+ cations involves 7 and 8 oxygen atoms, but due to the ionic character of the Rb–O interactions the bond lengths are diverse, making the geometry highly irregular and often distorted from ideal polyhedral shapes. The Rb centres in $Rb_3BTC{\cdot}5H_2O$ are linked by carboxylate groups into formally defined 2D SBUs, connected by BTC linkers into 3D network (Fig. 4). Finally, the SCXRD analysis of the $Rb_2HBTC{\cdot}3H_2O$ (space group $P\bar{1}$, Table S4) showed that all of the Rb centres are coordinated to 7 or 8 oxygen atoms. The SBU structure of $Rb_2HBTC{\cdot}3H_2O$ was similar to the material $K_2HBTC{\cdot}H_2O$ discussed above (Fig. 3), with 1D chain-type assembly parallel to the *a* crystallographic axis (Fig. 5a and b). However, the 1D SBUs in $Rb_2HBTC{\cdot}3H_2O$ are connected by the BTC ligands into 2D layers perpendicular to the *c* axis (Fig. 5c) forming a stacked supramolecular structure.

The accessibility of the developed Rb-based coordination networks using mechanochemical strategy was also investigated as an integral part of the study. To this end a series of mechanochemical reactions have been tested involving 2 : 1 and 3 : 1 stoichiometries and various reaction conditions (Table S5). As a result we found that both the $Rb_2HBTC{\cdot}3H_2O$ and $Rb_3BTC{\cdot}5H_2O$ phases can be prepared *via* DMF LAG (optimal for $Rb_2HBTC{\cdot}3H_2O$), EtOH LAG (optimal for $Rb_3BTC{\cdot}5H_2O$) or neat grinding (Fig. S5 and S6). Furthermore, similarly to the Na- and K-bases systems we have observed that the mechanochemical transformation from $Rb_2HBTC{\cdot}3H_2O$ to $Rb_3BTC{\cdot}5H_2O$ was easily achieved by milling the former with addition of RbOH and H_2O (1 : 1 : 1 molar ratio).

We would like to emphasise that the successful solid state preparation of $K_2HBTC{\cdot}H_2O$ and $Rb_2HBTC{\cdot}3H_2O$ demonstrates a valuable advantage of the mechanochemical approach over

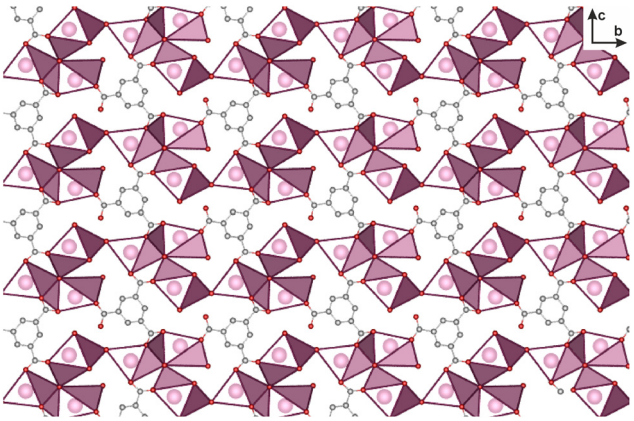

Fig. 4 Crystal structure of $Rb_3BTC{\cdot}5H_2O$. Rb = purple, O = red, C = grey, H atoms have been omitted for clarity. Single crystals of $Rb_3BTC{\cdot}5H_2O$ were prepared by exposition of aqueous Rb_3BTC solution to iPrOH vapours at RT.

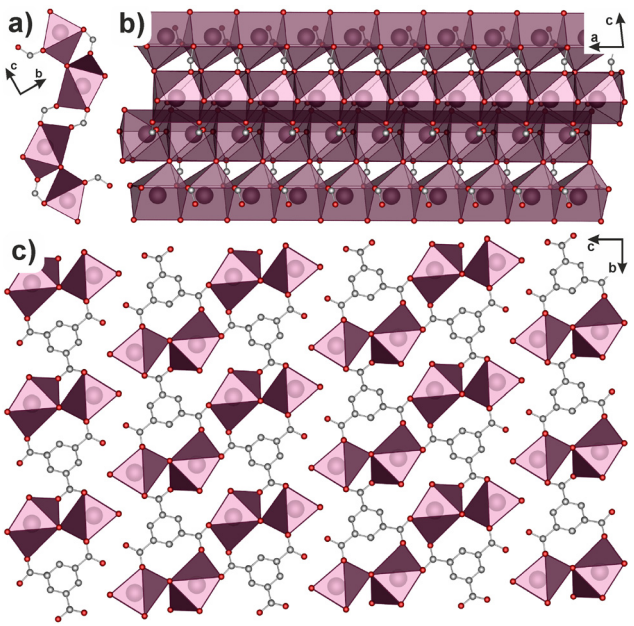

Fig. 5 Crystal structure of $Rb_2HBTC{\cdot}3H_2O$: 1D polymeric SBU (a and b), 2D coordination network (c). Rb = purple, O = red, C = grey, H atoms have been omitted for clarity. Single crystals of $Rb_2HBTC{\cdot}3H_2O$ were prepared by exposition of aqueous Rb_3BTC solution to EtOH vapours at RT.

the solution-base synthesis. The distinct reactivity observed among the alkali metal systems likely reflects the interplay between ionic size, solvation, and reaction environment. The selective formation of the M_2HBTC phases ($M = K^+$, Rb^+) under mechanochemical conditions may arise from the larger, less strongly solvated cations having a reduced tendency to stabilize the partially deprotonated $HBTC^{2-}$ species in solution. In contrast, Na^+, with its smaller ionic radius and higher hydration enthalpy, appears able to promote comparable deprotonation equilibria in aqueous media, thus allowing Na_2HBTC to form both in solution and in the solid state. Under solvent-free mechanochemical conditions, the absence of solvation equilibria and the direct acid–base interactions between H_3BTC and MOH constitute a fundamental difference in reaction environment; therefore, the formation of distinct phases compared to solution-based synthesis can be anticipated. While the direct reasons for the selective formation of the M_2HBTC phases under mechanochemical conditions are difficult to pinpoint, it may be speculated that mechanical treatment alters nucleation and crystal growth pathways by continuously renewing reactive surfaces, creating defects, and generating transient local temperature and pressure gradients.[53] These effects, combined with the absence of solvation equilibria and the non-equilibrium nature of the mechanochemical environment, can modify both the kinetic and thermodynamic profiles of the reaction.[54] As a result, mechanochemical synthesis may favour metastable intermediates or alternative phases that remain inaccessible under solution-based conditions.[55]

While the mechanochemical approach has been demonstrated to provide unmatched stoichiometric precision, it can also yield products of lower crystallinity or inferior properties. In order to examine this possibility, we have decided to investigate the thermal properties (using thermogravimetric analysis (TGA)), and crystal size and morphology (using SEM) of all of the materials discussed here. The TGA data (Fig. S7–S12) clearly show that the $M_3BTC{\cdot}xH_2O$ materials prepared by the solid state and solution methods exhibit very close thermal decomposition profiles with the only essential difference being the small weight loss (~2%) observed at around 380 °C for samples prepared in solid state. This observation might suggest minor contamination of the mechanochemically-prepared $M_3BTC{\cdot}xH_2O$ samples with the $M_2HBTC{\cdot}xH_2O$ phases, as the latter all displayed significant weight loss steps at around 380–400 °C (Fig. S7–S12). Notably, the decomposition steps observed around 100 °C for all of the samples matched the expected weight loss related to the transformation from the hydrated to dehydrated phase, which additionally confirms the composition of the investigated samples. Finally, we have employed SEM imaging technique in order to directly compare the crystal size and morphology of samples prepared using different methods. In general, the samples prepared *via* solution crystallisation consisted of well-defined crystals with average size from *ca.* 3–4 μm (for $Na_3BTC{\cdot}3H_2O$ and $K_3BTC{\cdot}3H_2O$, Fig. S13 and S16) to *ca.* 30–40 μm (for $Rb_3BTC{\cdot}5H_2O$, Fig. S20). Unsurprisingly, the mechanochemically-prepared samples displayed much smaller crystal size, mostly below 0.5 μm, but precise measurements were hindered by the irregular size of the crystallites (Fig. S14, S15, S17, S19, S21, S22). Nevertheless, we found that the limitations of the mechanochemical procedures can be mitigated by the post synthetic treatment, as demonstrated by the $K_3BTC{\cdot}3H_2O$ sample, which was subjected to aging (30 days) or DMF soaking (2 days) resulting in the enhanced phase purity and crystal size (Fig. S4c–e, S17 and S18).

Conclusions

In conclusion, we demonstrated that the seemingly simple alkali 1,3,5-benzenetricarboxylates can form a wide range of diverse structures in solid state involving products of various stoichiometry and hydration state. Importantly, all of the demonstrated materials were prepared using simple aqueous route and structurally characterized in detail using SCXRD technique. Moreover, we investigated the use of solvent-free mechanochemical strategy to prepare the developed alkali metal-based coordination networks, which revealed that most of them can be easily prepared by ball milling of 1,3,5-benzenetricarboxylic acid and respective alkali hydroxide for just *ca.* 20 minutes. Significantly, two of the reported alkali metal-based coordination networks ($K_2HBTC{\cdot}H_2O$ and $Rb_2HBTC{\cdot}3H_2O$) could only be prepared in high-yield using the mechanochemical approach. This selectivity reflects the superior stoichiometric control afforded by mechanochemical synthesis, which eliminates solvation equilibria and enables direct solid-state acid–base reactions between the components. In contrast to the solution synthesis, where cation size, solvation strength, and deprotonation equilibria govern the accessible phases, the mechanochemical route provides a pathway to phases that are thermodynamically or kinetically inaccessible in solution. In general, the demonstrated results indicate that mechanochemistry is not only a green alternative to traditional solution-based chemistry, but can also be a powerful tool for achieving precise stoichiometric and phase control in solid-state coordination chemistry. Overall, this comprehensive study offers a well-rounded insight into the synthesis and structural characteristics of alkali 1,3,5-benzenetricarboxylates. Further studies extending the scope to other organic linkers and transformations of alkali metal-based coordination polymers into functional porous carbons[35] are currently underway.

Conflicts of interest

There are no conflicts to declare.

Data availability

Supplementary information (SI): additional data concerning SCXRD, PXRD, TGA and SEM experiments. See DOI: https://doi.org/10.1039/d5dt01954k.

CCDC 2359250 ($Na_2HBTC{\cdot}3H_2O$), 2359252 ($K_2HBTC{\cdot}H_2O$), 2359487 ($Rb_2HBTC{\cdot}2H_2O$) and 2450580 ($Rb_3BTC{\cdot}5H_2O$) contain the supplementary crystallographic data for this paper.[56a–d]

Acknowledgements

The authors would like to acknowledge the financial support by the ENERGYTECH-1 project granted by the Warsaw University of Technology under the program Excellence Initiative: Research University (IDUB).

References

1 A. Porcheddu, E. Colacino, L. De Luca and F. Delogu, Metal-Mediated and Metal-Catalyzed Reactions Under Mechanochemical Conditions, *ACS Catal.*, 2020, **10**, 8344–8394.
2 R. T. O'Neill and R. Boulatov, The many flavours of mechanochemistry and its plausible conceptual underpinnings, *Nat. Rev. Chem.*, 2021, **5**, 148–167.
3 J. F. Reynes, F. Leon and F. García, Mechanochemistry for Organic and Inorganic Synthesis, *ACS Org. Inorg. Au*, 2024, **4**, 432–470.
4 F. García, M. Senna and V. Šepelák, Moving mechanochemistry forward: reimagining inorganic chemistry through mechanochemistry, *RSC Mechanochem.*, 2025, **2**, 499–502.
5 J. L. Howard, Q. Cao and D. L. Browne, Mechanochemistry as an emerging tool for molecular synthesis: what can it offer?, *Chem. Sci.*, 2018, **9**, 3080–3094.
6 A. Beillard, X. Bantreil, T.-X. Métro, J. Martinez and F. Lamaty, Alternative Technologies That Facilitate Access to Discrete Metal Complexes, *Chem. Rev.*, 2019, **119**, 7529–7609.
7 T. Tsuzuki, Mechanochemical synthesis of metal oxide nanoparticles, *Commun. Chem.*, 2021, **4**, 143.
8 D. Prochowicz, M. Saski, P. Yadav, M. Grätzel and J. Lewiński, Mechanoperovskites for photovoltaic applications: preparation, characterization, and device fabrication, *Acc. Chem. Res.*, 2019, **52**, 3233–3243.
9 F. Palazon, Y. El Ajjouri and H. J. Bolink, Making by Grinding: Mechanochemistry Boosts the Development of Halide Perovskites and Other Multinary Metal Halides, *Adv. Energy Mater.*, 2020, **10**, 1902499.
10 P. Li, F.-F. Cheng, W.-W. Xiong and Q. Zhang, New synthetic strategies to prepare metal–organic frameworks, *Inorg. Chem. Front.*, 2018, **5**, 2693–2708.
11 W. Wang, M. Chai, M. Y. B. Zulkifli, K. Xu, Y. Chen, L. Wang, V. Chen and J. Hou, Metal–organic framework composites from a mechanochemical process, *Mol. Syst. Des. Eng.*, 2023, **8**, 560–579.
12 J. M. Marrett, F. Effaty, X. Ottenwaelder and T. Friščic, Mechanochemistry for Metal–Organic Frameworks and Covalent–Organic Frameworks (MOFs, COFs): Methods, Materials, and Mechanisms, *Adv. Mater.*, 2025, 2418707.
13 S. Głowniak, B. Szczęśniak, J. Choma and M. Jaroniec, Mechanochemistry: Toward green synthesis of metal–organic frameworks, *Mater. Today*, 2021, **46**, 109–124.
14 T. Stolar and K. Užarević, Mechanochemistry: an efficient and versatile toolbox for synthesis, transformation, and functionalization of porous metal–organic frameworks, *CrystEngComm*, 2020, **22**, 4511–4525.
15 Z. Tegudeer, L. C. Davenport, M. E. Kordesch and W.-Y. Gao, Harnessing Mechanochemistry for Direct Synthesis of Imine-Based Metal–Organic Frameworks, *J. Am. Chem. Soc.*, 2025, **147**, 13522–13530.
16 M. Klimakow, P. Klobes, A. F. Thünemann, K. Rademann and F. Emmerling, Mechanochemical Synthesis of Metal–Organic Frameworks: A Fast and Facile Approach toward Quantitative Yields and High Specific Surface Areas, *Chem. Mater.*, 2010, **22**, 5216–5221.
17 M. Pilloni, F. Padella, G. Ennas, S. Lai, M. Bellusci, E. Rombi, F. Sini, M. Pentimalli, C. Delitala, A. Scano, V. Cabras and I. Ferino, Liquid-assisted mechanochemical synthesis of an iron carboxylate Metal Organic Framework and its evaluation in diesel fuel desulfurization, *Microporous Mesoporous Mater.*, 2015, **213**, 14–21.
18 D. Prochowicz, J. Nawrocki, M. Terlecki, W. Marynowski and J. Lewiński, Facile Mechanosynthesis of the Archetypal Zn-Based Metal–Organic Frameworks, *Inorg. Chem.*, 2018, **57**, 13437–13442.
19 D. Prochowicz, K. Sokołowski, I. Justyniak, A. Kornowicz, D. Fairen-Jimenez, T. Friščić and J. Lewiński, A mechanochemical strategy for IRMOF assembly based on pre-designed oxo-zinc precursors, *Chem. Commun.*, 2015, **51**, 4032–4035.
20 J. Nawrocki, D. Prochowicz, A. Wiśniewski, I. Justyniak, P. Goś and J. Lewiński, Development of an SBU–Based Mechanochemical Approach for Drug–Loaded MOFs, *Eur. J. Inorg. Chem.*, 2020, **2020**, 796–800.
21 Z. Nadizadeh, M. R. Naimi-Jamal and L. Panahi, Mechanochemical solvent-free in situ synthesis of drug-loaded $\{Cu_2(1,4\text{-bdc})_2(dabco)\}_n$ MOFs for controlled drug delivery, *J. Solid State Chem.*, 2018, **259**, 35–42.
22 L. E. Wenger and T. P. Hanusa, Synthesis without solvent: consequences for mechanochemical reactivity, *Chem. Commun.*, 2023, **59**, 14210–14222.
23 J. Beamish-Cook, K. Shankland, C. A. Murray and P. Vaqueiro, Insights into the Mechanochemical Synthesis of MOF-74, *Cryst. Growth Des.*, 2021, **21**, 3047–3055.
24 A. D. Katsenis, A. Puškarić, V. Štrukil, C. Mottillo, P. A. Julien, K. Užarević, M.-H. Pham, T.-O. Do, S. A. J. Kimber, P. Lazić, O. Magdysyuk, R. E. Dinnebier, I. Halasz and T. Friščić, In situ X-ray diffraction monitoring of a mechanochemical reaction reveals a unique topology metal-organic framework, *Nat. Commun.*, 2015, **6**, 6662.
25 J.-L. Do and T. Friščić, Mechanochemistry: A Force of Synthesis, *ACS Cent. Sci.*, 2017, **3**, 13–19.
26 G. Ayoub, B. Karadeniz, A. J. Howarth, O. K. Farha, I. Đilović, L. S. Germann, R. E. Dinnebier, K. Užarević and T. Friščić, Rational Synthesis of Mixed-Metal Microporous Metal–

Organic Frameworks with Controlled Composition Using Mechanochemistry, *Chem. Mater.*, 2019, **31**, 5494–5501.
27 V. Štrukil, L. Fábián, D. G. Reid, M. J. Duer, G. J. Jackson, M. Eckert-Maksić and T. Friščić, Towards an environmentally-friendly laboratory: dimensionality and reactivity in the mechanosynthesis of metal–organic compounds, *Chem. Commun.*, 2010, **46**, 9191.
28 G. A. Bowmaker, N. Chaichit, C. Pakawatchai, B. W. Skelton and A. H. White, Solvent-assisted mechanochemical synthesis of metal complexes, *Dalton Trans.*, 2008, 2926.
29 D. Banerjee and J. B. Parise, Recent advances in s-block metal carboxylate networks, *Cryst. Growth Des.*, 2011, **11**, 4704–4720.
30 K. M. Fromm, Coordination polymer networks with s-block metal ions, *Coord. Chem. Rev.*, 2008, **252**, 856–885.
31 M. A. Alnaqbi, A. Alzamly, S. H. Ahmed, M. Bakiro, J. Kegere and H. L. Nguyen, Chemistry and applications of s-block metal–organic frameworks, *J. Mater. Chem. A*, 2021, **9**, 3828–3854.
32 G. Ye, C. Chen, J. Lin, X. Peng, A. Kumar, D. Liu and J. Liu, Alkali /alkaline earth-based metal–organic frameworks for biomedical applications, *Dalton Trans.*, 2021, **50**, 17438–17454.
33 R. A. Smaldone, R. S. Forgan, H. Furukawa, J. J. Gassensmith, A. M. Z. Slawin, O. M. Yaghi and J. F. Stoddart, Metal-Organic Frameworks from Edible Natural Products, *Angew. Chem., Int. Ed.*, 2010, **49**, 8630–8634.
34 S. V. Dummert, H. Saini, M. Z. Hussain, K. Yadava, K. Jayaramulu, A. Casini and R. A. Fischer, Cyclodextrin metal–organic frameworks and derivatives: recent developments and applications, *Chem. Soc. Rev.*, 2022, **51**, 5175–5213.
35 M. Leszczyński, M. Kochaniec, M. Terlecki, I. Justyniak, S. A. Sahin, B. Aydogdu, R. Yuksel, M. Hołdyński, W. Wieczorek and J. Lewiński, Functional porous carbons derived from novel alkali metal-based coordination polymers for energy storage, *ChemRxiv*, 2025, preprint, DOI: DOI: 10.26434/chemrxiv-2025-ttn8k.
36 K. Jayaramulu, D. P. Dubal, B. Nagar, V. Ranc, O. Tomanec, M. Petr, K. K. R. Datta, R. Zboril, P. Gómez-Romero and R. A. Fischer, Ultrathin hierarchical porous carbon nanosheets for high–performance supercapacitors and redox electrolyte energy storage, *Adv. Mater.*, 2018, **30**, 1705789.
37 H. J. Kang, Y. H. Choi, I. W. Joo and J. E. Lee, Mechanochemical Synthesis of CD–MOFs and Application as a Cosmetic Ingredient, *Bull. Korean Chem. Soc.*, 2021, **42**, 737–739.
38 T. Grgurić, M. Razum, V. Martinez, G. Zgrablić, A. Senkić, B. Karadeniz, M. Etter, I. Brekalo, M. Arhangelskis, L. Pavić and K. Užarević, Green and Scalable Preparation of Highly Conductive Alkali Metal-dhta Coordination Polymers, *Inorg. Chem.*, 2024, **63**, 24587–24600.
39 I. Justyniak, W. Bury, D. Prochowicz, K. Wójcik, J. Zachara and J. Lewiński, Toward coordination polymers based on fine-tunable group 13 organometallic phthalates, *Inorg. Chem.*, 2014, **53**, 7270–7275.
40 M. K. Leszczyński, I. Justyniak, K. Gontarczyk and J. Lewiński, Solvent templating and structural dynamics of fluorinated 2D cu-carboxylate MOFs derived from the diffusion-controlled process, *Inorg. Chem.*, 2020, **59**, 4389–4396.
41 M. K. Leszczyński, A. Kornowicz, D. Prochowicz, I. Justyniak, K. Noworyta and J. Lewiński, Straightforward synthesis of single-crystalline and redox-active cr(II)-carboxylate MOFs, *Inorg. Chem.*, 2018, **57**, 4803–4806.
42 D. Ozer, D. A. Köse, O. Şahin and N. A. Oztas, Synthesis and characterization of boric acid mediated metal-organic frameworks based on trimesic acid and terephthalic acid, *J. Mol. Struct.*, 2017, **1141**, 261–267.
43 T.-T. Li, Y.-C. Qin and B.-K. Chen, The crystal structure of poly[(μ^{10}-5-carboxyisophthalato-κ^{10}O)disodium], $C_9H_4Na_2O_6$ *Z. Kristallogr. – New Cryst. Struct.*, 2020, **235**, 987–988.
44 M. K. Kim, V. Jo, D. W. Lee, I.-W. Shim and K. M. Ok, CAU-1 and CAU-2: New tubular alkali metal–organic framework materials, $A_3[C_6H_3(CO_2)(CO_2H_{0.5})(CO_2H)]_2$ (A = K or Rb), *CrystEngComm*, 2010, **12**, 1481.
45 P. Hayati, A. R. Rezvani, A. Morsali and P. Retailleau, Ultrasound irradiation effect on morphology and size of two new potassium coordination supramolecule compounds, *Ultrason. Sonochem.*, 2017, **34**, 195–205.
46 S.-F. Li, L. Hu, R.-L. Tang, Y. Ma, F.-F. Mao, J. Zheng, X.-D. Zhang and D. Yan, $KC_9H_5O_6(H_2O)$: A Promising UV Nonlinear-Optical Material with Large Birefringence Based on a π-Conjugated $(C_9H_5O_6)^-$ Group, *Inorg. Chem.*, 2022, **61**, 14880–14886.
47 D. R. Turner, J. Strachn-Hatton and S. R. Batten, Mono– and Di–Potassium Derivatives of Benzenepentacarboxylic Acid, *Z. Anorg. Allg. Chem.*, 2009, **635**, 439–444.
48 A. V. Pisareva, G. V. Shilov, Y. A. Dobrovolsky and A. I. Karelin, $Rb[C_6H_3(COOH)_2(COO–)] \cdot [C_6H_3(COOH)_3] \cdot 2H_2O$: Synthesis, Crystal Structure, and Properties, *Russ. J. Coord. Chem.*, 2004, **30**, 137–143.
49 Agilent Technologies, CrysAlisPro, *CrysAlisPro, Version 1.171.35.21b*.
50 G. M. Sheldrick, A short history of SHELX, *Acta Crystallogr., Sect. A:Found. Crystallogr.*, 2008, **64**, 112–122.
51 O. V. Dolomanov, L. J. Bourhis, R. J. Gildea, J. A. K. Howard and H. Puschmann, *OLEX2* : a complete structure solution, refinement and analysis program, *J. Appl. Crystallogr.*, 2009, **42**, 339–341.
52 L. J. Farrugia, *WinGX* and *ORTEP for Windows* : an update, *J. Appl. Crystallogr.*, 2012, **45**, 849–854.
53 A. A. L. Michalchuk, On the physical processes of mechanochemically induced transformations in molecular solids, *Chem. Commun.*, 2024, **60**, 14750–14761.
54 O. V. Lapshin, E. V. Boldyreva and V. V. Boldyrev, Role of Mixing and Milling in Mechanochemical Synthesis (Review), *Russ. J. Inorg. Chem.*, 2021, **66**, 433–453.
55 F. Cuccu, L. De Luca, F. Delogu, E. Colacino, N. Solin, R. Mocci and A. Porcheddu, Mechanochemistry: New Tools to Navigate the Uncharted Territory of "Impossible" Reactions, *ChemSusChem*, 2022, **15**, e202200362.

56 (*a*) CCDC 2359250: Experimental Crystal Structure Determination, 2025, DOI: 10.5517/ccdc.csd.cc2k5zvl; (*b*) CCDC 2359252: Experimental Crystal Structure Determination, 2025, DOI: 10.5517/ccdc.csd.cc2k5zxn; (*c*) CCDC 2359487: Experimental Crystal Structure Determination, 2025, DOI: 10.5517/ccdc.csd.cc2k67hj; (*d*) CCDC 2450580: Experimental Crystal Structure Determination, 2025, DOI: 10.5517/ccdc.csd.cc2n80zy.